DR THOMAS ALLEN SWIFT (Orcid ID : 0000-0003-1864-6523)

Article type : - Regular Manuscript

Photosynthesis and crop productivity are enhanced by glucose-functionalized carbon dots

Thomas A. Swift,[1,2,3] Daniel Fagan,[2] David Benito-Alifonso,[3] Stephen A. Hill,[3]
Marian L. Yallop,[2] Thomas A.A. Oliver,[1,3] Tracy Lawson,[4]
M. Carmen Galan[3]** and Heather M. Whitney[2]*

[1] Bristol Centre for Functional Nanomaterials, HH Wills Physics Laboratory, University of Bristol, BS8 1TL, UK

[2] School of Biological Sciences, Life Sciences Building, University of Bristol, BS8 1TQ, UK

[3] School of Chemistry, Cantock's Close, University of Bristol, BS8 1TS, UK

[4] School of Life Sciences, University of Essex, Colchester CO4 3SQ, UK

*Correspondence: Heather.Whitney@Bristol.ac.uk

**Correspondence: M.C.Galan@Bristol.ac.uk

Received: 21 April 2020

Accepted: 10 August 2020

ORCID

Thomas A. Swift[1,2,3] OrcID: 0000-0003-1864-6523

Daniel Fagan[2]
David Benito-Alifonso[3] OrcID: 0000-0002-5274-4875
Stephen A. Hill[3] OrcID: 0000-0001-5395-6426
Marian L. Yallop[2] OrcID: 0000-0001-9556-6389
Thomas A.A. Oliver[1,3] OrcID: 0000-0003-3979-7857
Tracy Lawson[4] OrcID: 0000-0002-4073-7221
M. Carmen Galan[3]** OrcID: 0000-0001-7307-2871
Heather M. Whitney[2]* OrcID: 0000-0001-6450-8266

Summary

- From global food security to textile production and biofuels, the demands currently made on plant photosynthetic productivity will continue to increase. Enhancing photosynthesis using designer, green and sustainable materials offers an attractive alternative to current genetic-based strategies and promising work with nanomaterials has recently started to emerge.
- Here we describe *in planta* use of carbon-based nanoparticles produced by low-cost renewable routes that are bioavailable to mature plants. Uptake of these functionalized nanoparticles directly from the soil improves photosynthesis and also increases crop production.
- We show for the first time that glucose-functionalization enhances nanoparticle uptake, photoprotection and pigment production, unlocking enhanced yields. This is demonstrated in *Triticum aestivum* 'Apogee' (dwarf bread wheat) and results in an 18% increase in grain yield.
- This establishes the viability of a functional nanomaterial to augment photosynthesis as a route to increased crop productivity.

Key words: carbon dots, crop productivity, food security, nanobionics, nanomaterials, photosynthesis, *Triticum aestivum*.

Introduction

Plants greatly underperform compared to the theoretical maximum photosynthetic efficiency. (Anten, 2005; Ort *et al.*, 2015) Even under moderate solar light intensities, plants often absorb light in excess

of that which can be safely harnessed due to downstream rate-limiting electron transport. Consequentially, plants take advantage of an inbuilt suite of photoprotective mechanisms, collectively termed non-photochemical quenching (NPQ), which dissipates excess energy and prevents deleterious photochemical reactions. (Melis, 2009) Whilst essential to plant survival, it is widely accepted that NPQ impacts the photosynthetic performance of many plant species, with recent studies demonstrating that transgenic modification that targeted reducing specific components of NPQ, or downstream molecular and enzymatic processes, resulted in a 15% increase of crop biomass. (Kromdijk *et al.*, 2016; Simkin *et al.*, 2017) While recent work has highlighted that nanoparticles (NPs) offer a promising method for enhancing photosynthesis, these studies have yet to achieve the significant desired increases in crop yield. (Giraldo *et al.*, 2014; Sai *et al.*, 2018; Kah *et al.*, 2019; Swift *et al.*, 2019; Li *et al.*, 2020; Xu *et al.*, 2020)

The work presented here accomplishes a dramatic increase in crop productivity by augmenting plants with specially engineered NPs. Here, the use of carbon dots (CDs) is explored to overcome the limitations of previously used nanomaterials such as toxicity, poor bioavailability or complex and inefficient syntheses, whilst retaining desirable properties such as being able to exchange electrons when photoexcited.(Giraldo *et al.*, 2014; Swift *et al.*, 2018, 2019) CDs are a carbon-based, fluorescent, small (less than 10 nm) class of nanoparticle. (Xu *et al.*, 2004; Baker & Baker, 2010; Hill & Galan, 2017; Swift *et al.*, 2018) Our team and others have previously demonstrated that glycan-surface functionalization of NPs mitigates acute toxicity and enhances internalization in mammalian cells. (Barras *et al.*, 2013; Reichardt *et al.*, 2013; Benito-Alifonso *et al.*, 2014; Hill *et al.*, 2016; Hill *et al.*, 2018; Swift *et al.*, 2018)

Herein we report the first example of glycan-functionalized CDs used to significantly increase grain yields of elite bread wheat by 18%. Our mechanistic investigations reveal that CD-photosynthetic interactions affects many facets of photosynthesis, and that glycan-functionalization of CDs is essential to realize improved yields by altering NPQ and pigment production whilst also reducing reactive oxygen species generation.

Materials and Methods

Statistics and significance

Data was initially analysed for significance using ANOVAs and p-values were calculated using the appropriate T-tests. 1, 2 or 3 asterisks are used throughout the manuscript to indicate a significant increase above the control of $P \leq 0.05$, $P \leq 0.01$ or $P \leq 0.001$ respectively. Additional details are given in the Supporting Information.

CD synthesis and characterization

Core CDs were synthesized following a modified procedure from our group.(Hill *et al.*, 2016; Swift *et al.*, 2018) The glucose-functionalized CDs were prepared via a two-step procedure starting from core-CDs. Briefly, treatment of core-CDs with succinic anhydride generated acid-coated CDs, that were then amide conjugated with 1-amino glucose, and subsequently purified through a 200 nm syringe filter and size-exclusion chromatography (Sephadex G-10, Sigma Aldrich) to yield the functionalized CDs (See Supporting Information for full experimental details). Glycan conjugation was performed with an excess of 1-amino glucose to ensure all the acid groups reacted. This solution was then stirred vigorously overnight. For storage, the glucose-CDs were dissolved in methanol and kept at 4˚C to prevent aggregation. See the Supporting Information and Fig. **S1** to Fig. **S7** for full details of the synthesis and characterization by NMR; Fourier transformed infrared spectroscopy; dynamic light scattering; absorbance spectroscopy and fluorescence spectroscopy.

Plant growth conditions and treatments

The plants were grown in compost (Levington, F2) in individual 10cmx10cm plots, in trays of 15 pots, and in a greenhouse at a constant 20.0 °C temperature. Natural Sun light (dynamically ranging from 100 to 800 μmol m^{-2} s^{-1}) was supplemented with LED lighting (PhytoLux, Attis-7) 80–120 μmol m^{-2} s^{-1} to provide a 16-hour photoperiod. From three weeks post germination until harvesting the plants were treated three times a week on Monday, Wednesday and Friday with 3.3 mg of treatment per plant (by adding 1L of 50mg/L treatment solution to each tray of 15 plants to be soaked up by the soil) totalling 10 mg of treatment per plant per week. The trays of pots were randomly rearranged and rotated three times a week on Monday, Wednesday and Friday. to compensate for any undetected differences in light or air quality across the greenhouse. Productivity measurements were made 10 weeks post germination at Zadoks stage 9.0–9.2 and after 7 weeks of treatment.

Fluorescence microscopy

Samples were imaged with a Leica DM200 and Leica MC120HD detector. Chlorophyll fluorescence was imaged using 470 nm excitation and the emission between 650–700 nm was collected, the CDs were imaged with a 365 nm excitation and 430–470 nm emission. Plants were selected for imaging from those available at random. Leaf tissues were dissected from the middle of flag leaves 7 weeks post-germination and after 4 weeks of treatment. To demonstrate the CD fluorescence, each treatment was imaged using the same excitation, microscope and detector settings. Histograms of the fluorescence observed across three images for each treatment across are given in Fig. **S9**. CDs were observed throughout the leaves but not in the grain of the plants.

Chlorophyll fluorescence and gas exchange measurements

A GFS-3000 (Waltz) and a MAXI-PAM (Waltz) were used for IRGA and chlorophyll fluorescence measurements respectively. Measurements were made at Zadoks 7.3–7.7 on flag leaves at seven weeks post germination. Plants were selected for measurements from those available at random. Plants were dark adapted for 40 minutes before light curve measurements. For chlorophyll fluorescence, the average across 10 equally sized areas evenly distributed across the leaf were recorded for each value. For the light curves the actinic light step length was 30 seconds. [CO_2] of 400 μmol mol^{-1}, [H_2O] of 17 mmol mol^{-1}, leaf temperature of 22 °C and vapour pressure deficit of 1.0 ± 0.2 kPa were all maintained for IRGA experiments.

Pigment measurements

Pigments were extracted from flag leaves and analysed by HPLC using previously developed methods.(Van Heukelem & Thomas, 2001) All solvents used were HPLC-grade. Samples were taken at the middle of the photoperiod on the same day, 0.1g of flag leaf was used for each sample, *N*=5. Plants were selected for measurements from those available at random. A stationary phase 3.5 μm spherical silica particle with an 80 Å pore size was used (Agilent, Eclipse XDB C8, 4.6 mm x 150 mm). Each of the peaks in the chromatogram were assigned by comparing their absorption spectrum

and elution time to known standards. Absorption wavelengths of 430 nm, 470 nm and 450 nm were used to quantify the concentrations of chlorophyll-*a*, chlorophyll-*b* and the carotenoids respectively.

Due to the dark adaption of the leaves no zeaxanthin or antheraxanthin were observed in the samples. It was not possible to separate α and β carotene, so peaks are simply labelled carotene however it is expected to be predominantly β-carotene.

Results

Synthesis of functionalized fluorescent CDs. Unfunctionalized amine-coated CDs (core-CDs) were synthesized in one-pot after three-minutes microwave heating of glucosamine·HCl and 4,7,10-Trioxa-1,13-tridecanediamine following a modified reported procedure. (Hill *et al.*, 2016; Swift *et al.*, 2018) Glucose-functionalization of the CDs was carried out in a two-step process by reaction of core-CDs with succinic anhydride to yield carboxylic acid bearing CDs, followed by N-(3-Dimethylaminopropyl)-N′-ethylcarbodiimide hydrochloride (EDC)-mediated conjugation of 1-aminoglucose to generate glucose-functionalized CDs (glucose-CDs) (Fig. **S1** to Fig. **S7**).

CDs uptake in plants.

The mechanisms by which the CDs interact with plants were investigated in *Triticum aestivum* treated with core-CDs or glucose-CDs and compared to untreated controls. Each of these CDs were applied directly to the soil from three weeks post germination. CD uptake from the soil was observed by fluorescence microscopy for both CD treatments, (Fig. **1**, Fig. **S8** and Table **S1**) which have a peak fluorescence intensity at 455 nm, (Swift *et al.*, 2018) and are spectrally isolated from chlorophyll emission. The CD uptake was quantified, yielding 29 ± 1 μg and 32 ± 1 μg per gram of leaf tissue for core and glucose CDs respectively. This measurement demonstrated that glucose-functionalization slightly enhances plant CD uptake ($N = 15$, $P < 0.05$, Supporting Information.)

Changes to *Triticum aestivum* biomass production.

The effect of uptake of CDs into the leaves on the physiology and yield were investigated, no toxic effects or responses were initially observed after treatment. The total ear mass per plant for glucose-CD treatments is 18% greater than control (P = 0.008, Fig. **2b**), whereas the core-CD treatment is not significantly different from the control (P = 0.4, Fig. **2b**). Glucose-CD treatment also increased the number of seeds produced by 12% (P = 0.02, Fig. **2c**) and shoot biomass by 17% (P = 0.02, Fig. **S10**). In all measurements, no significant effect was observed with treatment with glucose alone at the same concentrations (see SI).

Effect of CDs on photosynthetic performance in plants.

To investigate the origin of the observed yield increases, the effect of the CD-treatments on the photosynthetic performance of *Triticum aestivum* was investigated using standard protocols which measure chlorophyll fluorescence and infrared gas analysis (IRGA) as a function of photosynthetic photon fluence rate (PPFR). At high actinic-light intensities, a small but significant enhancement of the operating efficiency of Photosystem II (F_q'/F_m') was observed for both CD treatments (Fig. **3a**) compared to the control. Furthermore, we observed a significant decrease in NPQ for plants treated with glucose-CDs compared to the other samples (Fig. **3b**). Moreover, both CD treatments resulted in a significant increase of carbon assimilation (A) and the stomatal conductance (rate of CO_2 passage through stomata, g_s) compared to control ($P < 0.05$) for a wide range of PPFR (Fig. **3c** and Fig. **3d**). The A under saturating light conditions (A_{SAT}) and the maximum A (A_{MAX}) were extracted from exponential fits to data in Fig. **3c** and Fig. **S11**, respectively. The values for A_{SAT} and A_{MAX} for each treatment are given in Table **1**, with A_{MAX} invariant to CD treatment, but A_{SAT} enhanced by CD treatment.

The greater enhancement of carbon assimilation (A) compared to Photosystem II activity (F_q'/F_m') by treatment of plants with CDs, indicates that they alter processes downstream from the initial light harvesting, such as electron transport chain and stomatal efficiency, to enhance photosynthesis. (Lawson *et al.*, 2002) This hypothesis is supported by the increase in A_{SAT} upon addition of CDs, suggesting that the treated plants are able to perform more photochemistry with the light that they absorb, *e.g.* an increased operational efficiency, but do not enhance the maximum photosynthetic capacity of plants, since A_{MAX} is unaffected.

Kinetics of photosynthetic performance.

We then focused on the response of the treated plants to changes in light conditions by measuring the induction and relaxation of A, g_s, F_q'/F_m' and NPQ. These measurements were performed as dark-light-dark cycles as displayed in Fig. **4**. The induction of stomatal conductance was fitted using a previously developed model (McAusland *et al.*, 2016) to quantify the maximum rate of stomatal conductance (Sl_{MAX}) upon exposure to light. These experiments revealed that Sl_{MAX} increased for both the CD treatments, Fig. **4b**.

To quantify the relaxation of NPQ upon re-adaptation to dark conditions, the curves for 70-130 mins in Fig. **4d** were fitted to bi-exponential decays, as per previous studies, (Kromdijk *et al.*, 2016) and tabulated in Table 1. Relative to the control, the rapid component of NPQ relaxation (NPQ_1) was sped up by the core-CD treatment, yet glucose-CD treatment slowed down NPQ_1. We tested if this increase could relate to a relative reduction in the available carotenoid pigments which contribute to the fastest NPQ component,(Kromdijk *et al.*, 2016; Leuenberger *et al.*, 2017) Fig. **4d** (and pigment ratio analysis supported this view- see Fig. **5** and discussion below). The relaxation of the secondary component (NPQ_2), was slower (*e.g.* longer lifetime) for the core-CD treatment compared to the untreated control, implying a greater photoinhibition which results in increased photodamage by the core-CD treatment, whereas NPQ_2 was accelerated by the glucose-CD treatment, indicative of less photodamage- see Table 1.

Effect of CD treatment on Pigment Composition.

The effect of CD treatment on the pigment composition was further investigated by the extraction and quantification of light harvesting and photoprotective pigments by high-performance liquid chromatography (HPLC), see Fig. **5** and Fig. **S12**. No significant differences in pigment ratios were observed between the untreated control and core-CD treatments. Conversely, for the glucose-CD treatment an increase in the ratio of chlorophylls to carotenoids, chlorophyll-*a* to chlorophyll-*b* and chlorophyll-*a* to lutein were observed compared to control and core-CD treatments. The increase in the ratio of chlorophyll-*a* to lutein supports the earlier conclusion that a reduced carotenoid pool in glucose-CDs treated plants slows NPQ_1, however, there are other processes that could affect NPQ_1 (Nilkens *et al.*, 2010; Demmig-Adams *et al.*, 2014). By contrast no effect was observed on the ratio of chlorophyll-*a* to violaxanthin for either CD treatment. In general, the glucose-CD treatment results in an increased production of light harvesting pigments compared to photoprotective pigments which suggests that glucose-CD treatment enables the plants to maintain reduced levels of photoprotection compared to the control or core-CD treatment.

The effects of the reduced photoprotection for the glucose-CD treatment were further investigated by measuring reactive oxygen species (ROS) production by illumination of chloroplasts isolated from untreated plants that were then treated with CDs. Core-CDs were observed to increase ROS production compared to the untreated control (Fig. **S13**), however, little effect was observed in the case of the glucose-CD treated chloroplasts, despite the glucose-CD treated plants producing fewer photoprotective pigments and performing less NPQ (see Fig. **4** and Fig. **5**). This suggests that the core-CD treatment results in increased photodamage compared to the control, but this is prevented by the glucose-functionalization of the CDs.

Discussion

Our results demonstrate that by utilizing biomolecule functionalized CDs it is possible to realize increased crop yields. While previous studies with CDs might have provided a route to the beneficial effect of enhancing photosynthesis, none have resulted in significant increased crop productivity: in

agreement with what is observed with the unfunctionalized core-CD treatment in this study.(Chandra *et al.*, 2014; Li *et al.*, 2016; Xu *et al.*, 2020) This accentuates the need to design the functional surface of NPs for biological applications. The greater increase of A in comparison to F_q'/F_m' observed in this paper agrees with the hypothesis previously proposed by Chandra *et al.* that CDs primarily enhance the electron transport in the thylakoid membranes, resulting in augmented photosynthesis rather than acting as optical amplifiers as recently reported by Xu *et al.*(Chandra *et al.*, 2014; Xu *et al.*, 2020) The CD are most likely able to enhanced electron transport because of their ability to easily exchange electrons when photoexcited.(Swift *et al.*, 2018) Enhanced electron transport between the photosystems also explains the comparative reduction in NPQ for the glucose-CD treatment at high irradiance as more electrons can be directed to photochemistry. This effect is present in both the core-CD and glucose-CD treatments however it is mitigated in the core-CD treatment by an increase in ROS production, explaining the observed difference in crop yield between the core-CD and glucose-CD treatments. The glucose-CD treatment is able to capitalise on the increased electron transport and chlorophyll production and decrease lutein production which results in an enlarged photosynthetic capacity, whilst the core-CD treatment is limited by ROS production. These disparities between the core-CD and glucose-CD treatments are exacerbated by the enhanced uptake and internalisation into the mesophyll cells for the glucose-CD treatment.

The methods demonstrated here provide a renewable, low-cost and facile route to an increase in *Triticum aestivum* productivity of 18% using functional nanomaterials. If we are to address the increase in crop productivity to meet forecast global food demand in the future, (Zhu *et al.*, 2010; Ray *et al.*, 2013; Tilman & Clark, 2015; Kromdijk & Long, 2016) one potential route could be to embrace the use of nanomaterials to enhance yields. The use of designer-NPs has the potential to be combined with previously demonstrated transgenic techniques to bring crop productivity towards a theoretical maximum. These new techniques could also be applied to biofuels, biomass and bio-photovoltaics with the potential to enhance green-energy production.

We have demonstrated the use of glycan-functionalized nanomaterials to obtain an increase in the yield of crop, that has eluded previous studies.(Giraldo *et al.*, 2014; Xu *et al.*, 2020) These materials also exhibit high bio-availability enabling simple treatment on a larger scale providing a significant advantage over previous methods. The synthetic routes used to access the nanomaterials

are simple and sustainable. As a consequence, we believe this work represents a step towards the use of designer nanomaterials for agricultural applications.

Acknowledgements

We would like to thank Tom Pitman, Alanna Kelly and Anna Lim (University of Bristol) for growing the plants; Taryn Fletcher (University of Bristol) for her help with experimental work; and James Stevens (University of Essex) for his advice on IRGA measurements. This research was supported by EPSRC-BCFN PhD studentship EP/G036780/1 and EPSRC Doctoral Prize fellowship EP/R513179/1 (TAS); EPSRC CAF EP/J002542/1 and ERC-COG:648239 (MCG); NERC grant NE/N006518/1 (MLY, DF); BBSRC grants BB/N016831/1 & BB/N021061/1 (TL), Royal Society University Research Fellowship UF1402310 (TAAO), the Bristol Centre for Agricultural Innovation and the Wolfson Foundation. The concepts of the paper are shared with a patent filed by the University of Bristol: International (WO) Patent Application No: PCT/EP2018/097143 on which TAS, DBA, MCG and HMW are named inventors.

Author Contributions

TAS, MLY, TAAO, MCG, TL and HMW conceived the experiments; TAS carried out the microscopy, chlorophyll fluorescence, CD-pigment interactions, IRGA and physiology experiments; TAS and DF performed the HPLC; DBA developed the modified synthesis; SAH created the original synthesis; TAS synthesized and characterized the CDs; and TAS, TAAO, HMW and MCG co-wrote the manuscript, which all authors commented on and edited.

References

Anten NPR. **2005**. Optimal photosynthetic characteristics of individual plants in vegetation stands and implications for species coexistence. *Annals of Botany* **95**: 495–506.

Baker SN, Baker GA. **2010**. Luminescent Carbon Nanodots: Emergent Nanolights. *Angewandte Chemie International Edition* **49**: 6726–6744.

Barras A, Martin FA, Bande O, Baumann J-S, Ghigo J-M, Boukherroub R, Beloin C, Siriwardena A, Szunerits S. **2013**. Glycan-functionalized diamond nanoparticles as potent *E. coli* anti-adhesives. *Nanoscale* **5**: 2307–2316.

Benito-Alifonso D, Tremel S, Hou B, Lockyear H, Mantell J, Fermin DJ, Verkade P, Berry M, Galan MC. **2014**.

Lactose as a "Trojan Horse" for Quantum Dot Cell Transport. *Angewandte Chemie International Edition* **53**: 810–814.

Chandra S, Pradhan S, Mitra S, Patra P, Bhattacharya A, Pramanik P, Goswami A. **2014**. High throughput electron transfer from carbon dots to chloroplast: a rationale of enhanced photosynthesis. *Nanoscale* **6**: 3647–55.

Demmig-Adams B, Gyözö G, Adams III W, Govindjee. **2014**. *Non-Photochemical Quenching and Energy Dissipation in Plants, Algae and Cyanobacteria* (B Demmig-Adams, G Garab, W Adams III, and Govindjee, Eds.). Dordrecht: Springer Netherlands.

Giraldo JP, Landry MP, Faltermeier SM, McNicholas TP, Iverson NM, Boghossian A a, Reuel NF, Hilmer AJ, Sen F, Brew J a, *et al.* 2014. Plant nanobionics approach to augment photosynthesis and biochemical sensing. *Nature Materials* **13**: 400–408.

Van Heukelem L, Thomas CS. **2001**. Computer-assisted high-performance liquid chromatography method development with applications to the isolation and analysis of phytoplankton pigments. *Journal of Chromatography A* **910**: 31–49.

Hill SA, Benito-Alifonso D, Davis SA, Morgan DJ, Berry M, Galan MC. **2018**. Practical Three-Minute Synthesis of Acid-Coated Fluorescent Carbon Dots with Tuneable Core Structure. *Scientific Reports* **8**: 12234.

Hill SA, Benito-Alifonso D, Morgan DJ, Davis SA, Berry M, Galan MC. **2016**. Three-minute synthesis of sp 3 nanocrystalline carbon dots as non-toxic fluorescent platforms for intracellular delivery. *Nanoscale* **8**: 18630–18634.

Hill SA, Galan MC. **2017**. Fluorescent carbon dots from mono- and polysaccharides: synthesis, properties and applications. *Beilstein Journal of Organic Chemistry* **13**: 675–693.

Kah M, Tufenkji N, White JC. **2019**. Nano-enabled strategies to enhance crop nutrition and protection. *Nature Nanotechnology* **14**: 532–540.

Kromdijk J, Głowacka K, Leonelli L, Gabilly ST, Iwai M, Niyogi KK, Long SP. **2016**. Improving photosynthesis and crop productivity by accelerating recovery from photoprotection. *Science* **354**: 857–861.

Kromdijk J, Long SP. **2016**. One crop breeding cycle from starvation? How engineering crop photosynthesis for rising CO 2 and temperature could be one important route to alleviation. *Proceedings of the Royal Society B: Biological Sciences* **283**: 20152578.

Lawson T, Oxborough K, Morison JIL, Baker NR. **2002**. Responses of photosynthetic electron transport in stomatal guard cells and mesophyll cells in intact leaves to light, CO_2, and humidity. *Plant Physiology* **128**: 52–62.

Leuenberger M, Morris JM, Chan AM, Leonelli L, Niyogi KK, Fleming GR. **2017**. Dissecting and modeling zeaxanthin- and lutein-dependent nonphotochemical quenching in *Arabidopsis thaliana*. *Proceedings of the National Academy of Sciences of the United States of America* **114**: E7009–E7017.

Li Y, Xu X, Wu Y, Zhuang J, Zhang X, Zhang H, Lei B, Hu C, Liu Y. **2020**. A review on the effects of carbon dots in plant systems. *Materials Chemistry Frontiers* **4**: 437–448.

Li W, Zheng Y, Zhang H, Liu Z, Su W, Chen S, Liu Y, Zhuang J, Lei B. **2016**. Phytotoxicity, Uptake, and Translocation of Fluorescent Carbon Dots in Mung Bean Plants. *ACS Applied Materials & Interfaces* **8**: 19939–19945.

McAusland L, Vialet-Chabrand S, Davey P, Baker NR, Brendel O, Lawson T. **2016**. Effects of kinetics of light-induced stomatal responses on photosynthesis and water-use efficiency. *New Phytologist* **211**: 1209–1220.

Melis A. **2009**. Solar energy conversion efficiencies in photosynthesis: Minimizing the chlorophyll antennae to maximize efficiency. *Plant Science* **177**: 272–280.

Nilkens M, Kress E, Lambrev P, Miloslavina Y, Müller M, Holzwarth AR, Jahns P. **2010**. Identification of a slowly inducible zeaxanthin-dependent component of non-photochemical quenching of chlorophyll fluorescence generated under steady-state conditions in *Arabidopsis*. *Biochimica et Biophysica Acta* **1797**: 466–75.

Ort DR, Merchant SS, Alric J, Barkan A, Blankenship RE, Bock R, Croce R, Hanson MR, Hibberd JM, Long SP, *et al.* 2015. Redesigning photosynthesis to sustainably meet global food and bioenergy demand. *Proceedings of the National Academy of Sciences of the United States of America* **112**: 8529–8536.

Ray DK, Mueller ND, West PC, Foley JA. **2013**. Yield Trends Are Insufficient to Double Global Crop Production by 2050. (JP Hart, Ed.). *PloS one* **8**: e66428.

Reichardt NC, Martín-Lomas M, Penadés S. **2013**. Glyconanotechnology. *Chemical Society Reviews* **42**: 4358–4376.

Sai L, Liu S, Qian X, Yu Y, Xu X. **2018**. Nontoxic fluorescent carbon nanodot serving as a light conversion material in plant for UV light utilization. *Colloids and Surfaces B: Biointerfaces* **169**: 422–428.

Simkin AJ, Lopez-Calcagno PE, Davey PA, Headland LR, Lawson T, Timm S, Bauwe H, Raines CA. **2017**. Simultaneous stimulation of sedoheptulose 1,7-bisphosphatase, fructose 1,6-bisphophate aldolase and the photorespiratory glycine decarboxylase-H protein increases CO_2 assimilation, vegetative biomass and seed yield in *Arabidopsis*. *Plant Biotechnology Journal*: 1–12.

Swift TA, Duchi M, Hill SA, Benito-Alifonso D, Harniman RL, Sheikh S, Davis SA, Seddon AM, Whitney HM, Galan MC, Oliver TAA. 2018. Surface functionalisation significantly changes the physical and electronic properties of carbon nano-dots. *Nanoscale* **10**: 13908–13912.

Swift TA, Oliver TAA, Galan MC, Whitney HM. **2019**. Functional nanomaterials to augment photosynthesis: evidence and considerations for their responsible use in agricultural applications. *Interface Focus* **9**: 20180048.

Tilman D, Clark M. **2015**. Food, Agriculture And the Environment: Can We Feed the World And Save the Earth? *Daedalus* **144**: 8–23.

Xu X, Mao X, Zhuang J, Lei B, Li Y, Li W, Zhang X, Hu C, Fang Y, Liu Y. **2020**. PVA-Coated Fluorescent Carbon Dot Nanocapsules as an Optical Amplifier for Enhanced Photosynthesis of Lettuce. *ACS Sustainable Chemistry and Engineering* **8**: 3938–3949.

Xu X, Ray R, Gu Y, Ploehn HJ, Gearheart L, Raker K, Scrivens WA. **2004**. Electrophoretic Analysis and Purification of Fluorescent Single-Walled Carbon Nanotube Fragments. *Journal of the American Chemical Society* **126**: 12736–12737.

Zhu XG, Long SP, Ort DR. **2010**. Improving photosynthetic efficiency for greater yield. *Annual Review of Plant Biology* **61**: 235–261.

Supporting Information

Additional Supporting Information may be found online in the Supporting Information section at the end of the article.

Table 1. Calculated photosynthetic parameters in *Triticum aestivum.*

Parameter	Treatment		
	Control	Core-CD	Glucose-CD
A_{SAT} (μmol m^{-2} s^{-1})	22.0 ± 0.8	24.0 ± 0.9	24.0 ± 0.9
A_{MAX} (μmol m^{-2} s^{-1})	31 ± 2	31 ± 1	30 ± 1
Sl_{MAX} (μmol m^{-2} s^{-2})	222 ± 6	336 ± 4	244 ± 7
Amplitude of NPQ_1	0.574 ± 0.008	0.50 ± 0.01	0.71 ± 0.01
τ_1 (s)	85 ± 3	72 ± 5	94 ± 3
Amplitude of NPQ_2	0.42 ± 0.04	0.502 ± 0.004	0.29 ± 0.03
τ_2 ($\times 10^3$ s)	7 ± 2	10.3 ± 0.4	3.0 ± 0.6

Values obtained from fits to infrared gas analysis (IRGA) and chlorophyll fluorescence measurements. Sl_{MAX} is the maximum rate of stomatal opening calculated from Fig. **4b**. The amplitudes of NPQ_1 and NPQ_2 are the proportions of fast and slow non-photochemical quenching (NPQ) relaxation respectively with their associated lifetimes τ_1 and τ_2 as calculated from Fig. **4d**. Errors given are the 95% confidence bounds of fitting, $r^2 \geq 0.9737$ for all fits.

Fig. 1 Fluorescence microscopy of CDs in *Triticum aestivum* mesophyll. Tissues were taken from the fully expanded flag-leaves. An increase in fluorescence intensity was observed for the CD treatments (core- and glucose-CD) when compared to untreated controls. All images are the displayed on the same scale, with the white scale bar representing 100 μm. Fluorescence intensities are also displayed on the same scale. Schematics of the structure of the NP treatments are simplified and not to scale. Images were collected with 365 nm excitation (resonant with CD) and 455 nm emission.

Fig. 2 Physiology and yield measurements in *Triticum aestivum.* (**a**) Image of the dried, threshed seed yield after treatments. For each box the red central line indicates the median, the blue top edges indicate the 25th percentile, the blue bottom edge indicates the 75th percentile, the whiskers indicate the range excluding outliers, red squares indicate outliers. Black asterisks indicate a difference from the control, blue asterisks indicate a difference between the core and glucose CD treatments. 1, 2 or 3 asterisks are used to indicate $P \leq 0.05$, $P \leq 0.01$ or $P \leq 0.001$ respectively. (**a**) N=32, for (**b**, **c** and **f**) N=36, 32 and 36 for the control, core-CD and glucose-CD treatments, respectively; (**d**) N=35, 32 and 35 for the control, core-CD and glucose-CD treatments, respectively and (**e**) N=9. Additional tables of statistical parameters are given in the Supporting Information (Tables S2 and S3).

Fig. 3 Irradiance dependent photosynthetic performance of *Triticum aestivum*. Light curves for (**a**) Photosystem II operating efficiency (F_q'/F_m'); (**b**) non-photochemical quenching (NPQ); (**c**) carbon assimilation (A); (**d**) stomatal conductance(g_s). Values are obtained from chlorophyll fluorescence (**a**, **b**) and infrared gas analysis (IRGA, **c**, **d**) measurements of the three different treatments. The light curve was fitted with an exponential model. The values of A under saturating light conditions (A_{SAT}) are given in the Table 1. $r^2 \geq 0.9945$ for all fits. Red or blue asterisks are used to indicate a difference between the core-CD treatment and the control or the glucose-CD treatment and control respectively. 1, 2 or 3 asterisks are used to indicate $P \leq 0.05$, $P \leq 0.01$ or $P \leq 0.001$ respectively.

Fig. 4 Kinetics of photosynthetic performance in *Triticum aestivum*. Adaptation kinetics for (**a**) carbon assimilation (A); (**b**) stomatal conductance (g_s), the maximum rate of g_s (Sl_{MAX}) values were fitted using a previously developed model (McAusland et al., 2016)); (**c**) photosystem II operating efficiency (F_q'/F_m'); (**d**) non-photochemical quenching (NPQ) kinetics where the relaxation of NPQ was fitted with a bi-exponential decay. (Kromdijk et al., 2016) The periods of dark and light are indicated with black and white boxes

respectively. Light corresponds to a photosynthetic-photon fluence rate (PPFR) of 1000 μmol m^{-2} s^{-1} and dark corresponds to a PPFR of 0 μmol m^{-2} s^{-1} for (**c**, **d**) and 100 μmol m^{-2} s^{-1} for (**a**, **b**). N=5 except for the control in (3a, 3b) where N=4. Calculated values are given in Table 1 and additional details are given in the Materials and Methods section.

Fig. 5 Photosynthetic pigment ratios in *Triticum aestivum*. Pigment ratios extracted by high-performance liquid-chromatography (HPLC) from treated plants. Black asterisks indicate a difference from the untreated control, blue asterisks indicate a difference between the core and glucose CD treatments. 1, 2 or 3 asterisks are used to indicate $P \leq 0.05$, $P \leq 0.01$ or $P \leq 0.001$ respectively. Only the glucose-CDs demonstrated a significant difference from the control. N=5, additional tables of statistical parameters is given in the Supporting Information (Tables S4 and S5).

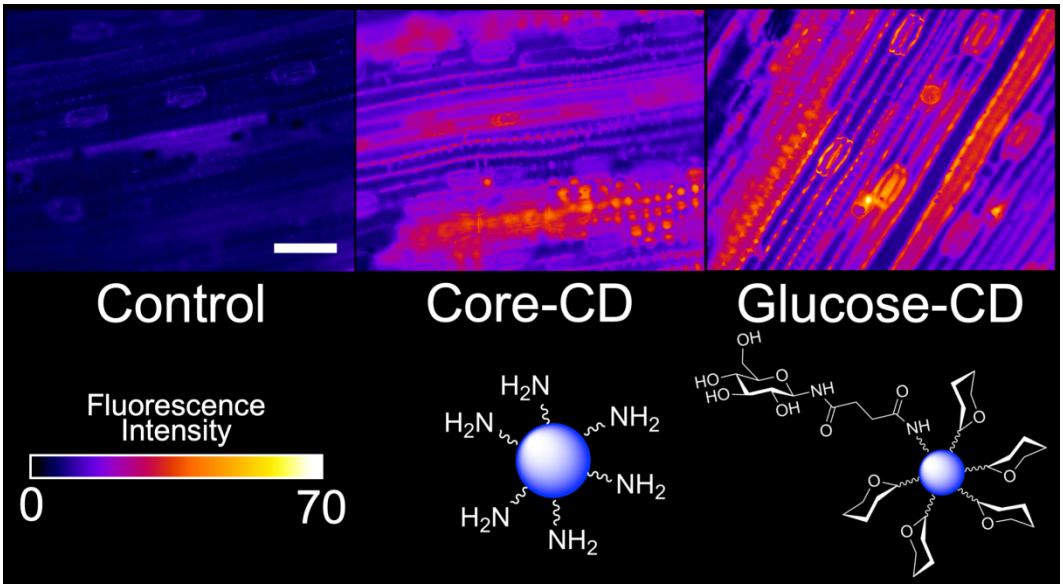

nph_16886_f1.png

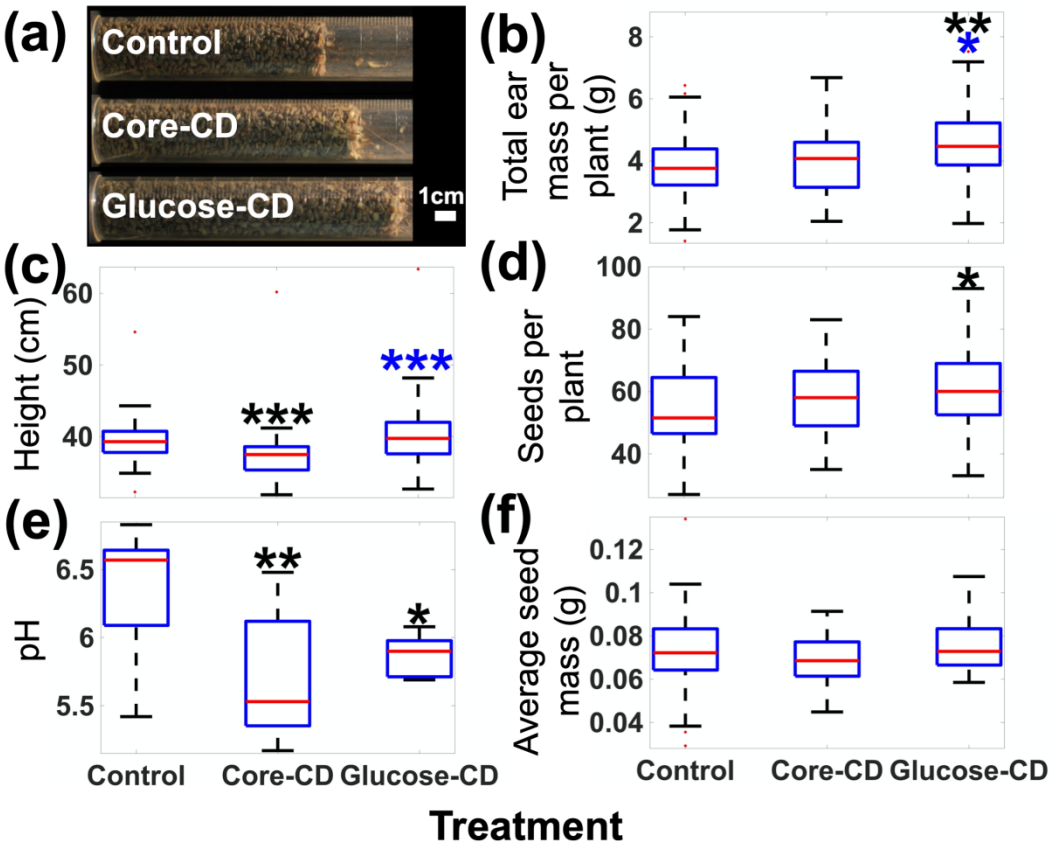

nph_16886_f2.png

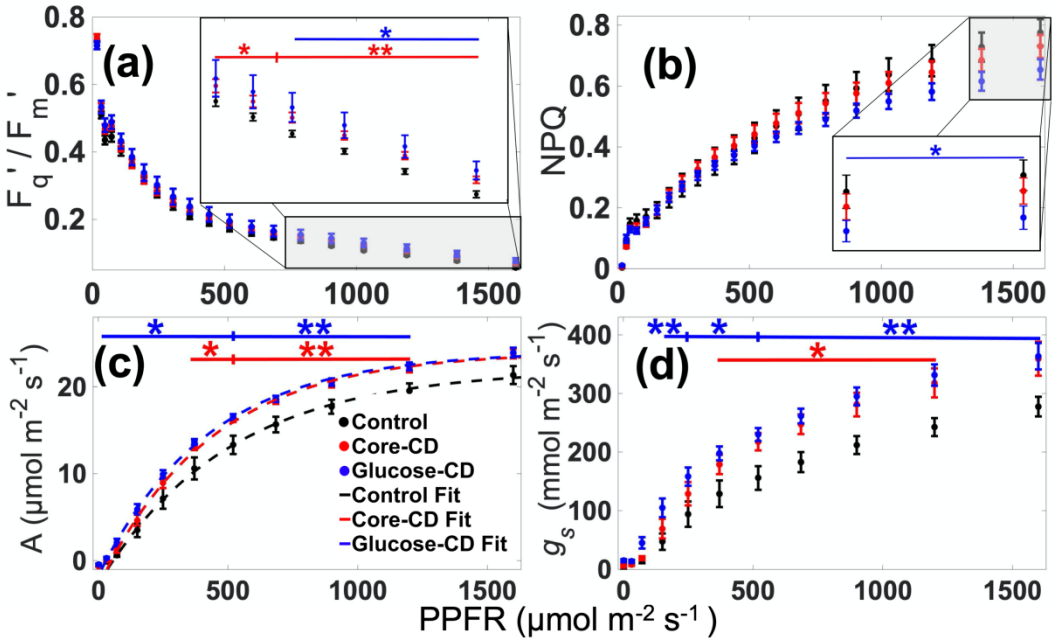

nph_16886_f3.png

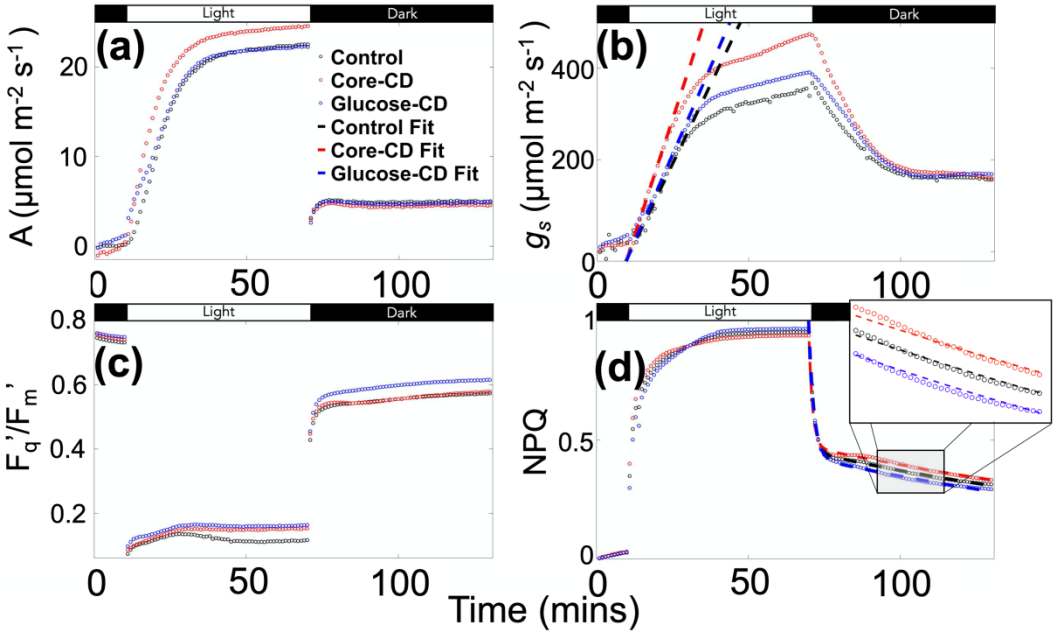

nph_16886_f4.png

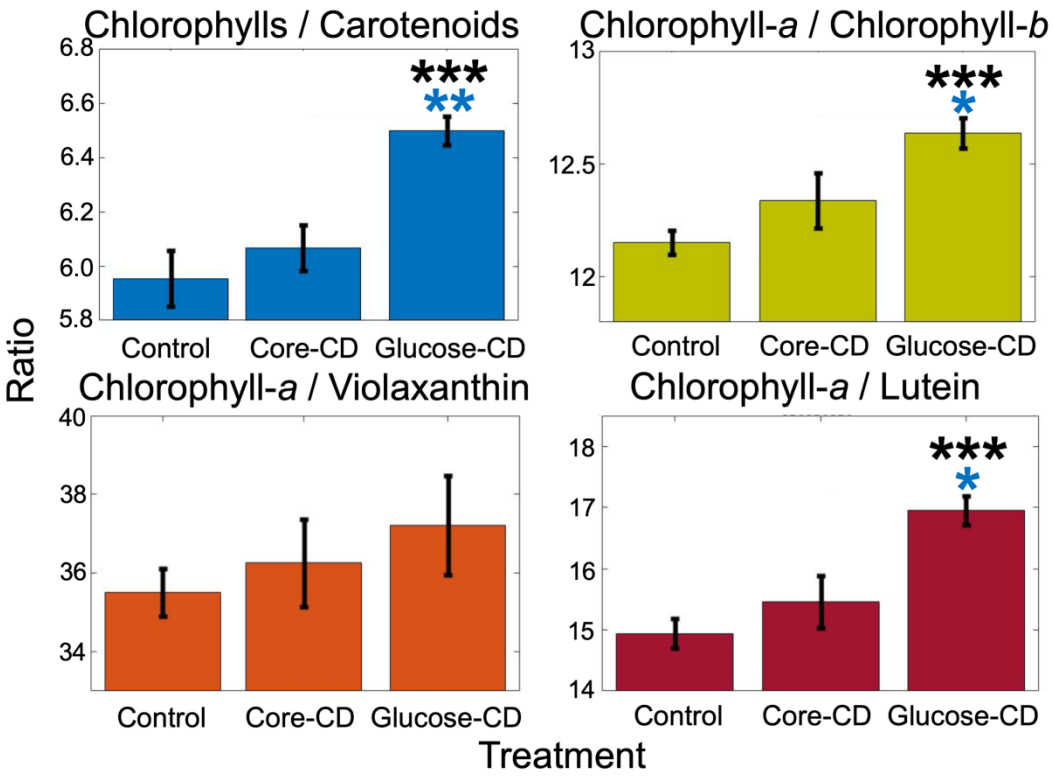

nph_16886_f5.png